

Original Article

CT and MRI manifestations of peripheral primitive neuroectodermal tumors

Bin Song, Hao Wang, Ran Wei

Department of Radiology, Minhang Branch, Zhongshan Hospital, Fudan University, Shanghai City, P. R. China

Received June 3, 2018; Accepted June 28, 2018; Epub September 15, 2018; Published September 30, 2018

Abstract: Objective: To investigate CT and MRI features of peripheral primitive neuroectodermal tumors (pPNETs). Methods: Clinical data of 16 patients with pPNETs confirmed by surgical resection who were admitted to The Minhang Branch of Zhongshan Hospital from January 2010 to December 2017 were retrospectively reviewed. Among those patients, 8 underwent CT scan and 8 underwent MRI scan. The enrolled patients were analyzed for their lesion distribution, diagnosis profiles, CT and MRI features, results of pathological examination, and recurrence and metastasis. Results: Surgical pathological examination was done on 16 patients that met the criteria for pathological examination of pPNETs. CT images showed pPNETs of soft tissue were lesions which had uneven internal structure density and ill-defined margins, accompanied by cystic degeneration or necrosis, but no calcification. Enhanced CT scans showed heterogeneous enhancement. MRI images demonstrated that the tumors were isointense or slightly hypo-intense in T1 weighted scan, and they were heterogeneously hyper-intense or slightly hyper-intense in T2 weighted scan. Necrotic or cystic lesions showed changes of longer T1 and long T2 signals. Enhanced scan presented homogeneous or heterogeneous enhancement. The CT images showed pPNETs of bone tissue were lesions which had osteolytic bone destruction with ill-defined margins, no periosteal reaction, with or without surrounding soft-tissue masses of varying degrees. MRI images revealed that the lesions had disruption of the cortical bone signals in the disrupted region, and changes in signals in the medullary cavity and surrounding soft tissue. The lesions showed slightly hypo-intense or iso-intense signals on T1 weighted images, hyper-intense or slightly hyper-intense signals on the T2 weighted images, and heterogeneous signals after enhancement. Results of follow-up post-surgery indicated that 3 patients had recurrence of primary lesions, whereas 2 had pulmonary metastases, 3 had bone metastases, 1 had intracranial metastasis, and 6 had no recurrence or metastasis. Conclusion: pPNETs showed no specific CT and MRI features, but the disease could be diagnosed by analyzing the extent of tumor involvement, recurrence, and metastasis based on the findings of CT or MRI studies. CT and MRI features provide reference value for diagnosis differentiation, surgical protocol planning, efficacy evaluation and prognosis.

Keywords: Peripheral primitive neuroectodermal tumors, CT, MRI, imaging feature

Introduction

Peripheral primitive neuroectodermal tumors (pPNETs) are malignant tumors with cytological and cellular genetic features that are present in the extracranial skeletal system or soft tissue. They originate from the neuroectoderm and consist of primitive undifferentiated small round cells [1-3]. An epidemiological study on pPNETs revealed that the disease accounts for only 4% of all soft-tissue sarcomas, and children and adolescents are a high-risk population [4]. However, few reports focused on the radiological findings of pPNETs, and misdiagnosis of the disease is common in clinical practice

[5]. In recent years, with the advance in research on clinical and pathological features of pPNETs, more relevant reports are available [6-8]. Nevertheless, CT and MRI features of pPNETs are still indefinite, which is not helpful to improve diagnosis of the disease and cannot provide imaging basis for planning protocols of surgical resection [9, 10]. As a result, in this study CT and MRI features of pPNETs were investigated and shown to be important supplements in diagnosis of the disease. Therefore, a retrospective analysis was conducted regarding the clinical data of 16 patients with surgically and pathologically confirmed pPNETs who admitted to The Minhang Branch of Zhongshan

CT and MRI features of peripheral primitive neuroectodermal tumors

Table 1. Basic characteristics of 16 pPNETs patients

Variable	Value
Sex (n)	6/10
Age (year)	18.6 ± 2.5
Course of disease (mon)	6.1 ± 1.4
Tumor volume (cm ³)	10.4*6.7*5.1
Age distribution (n)	
<10 years old	1
10-30 years old	9
30-50 years old	3
>50 years old	3
Tumor with well-defined margins (n)	7
Tumor with ill-defined margins (n)	9
Solitary tumor (n)	11
Multiple tumor (n)	5

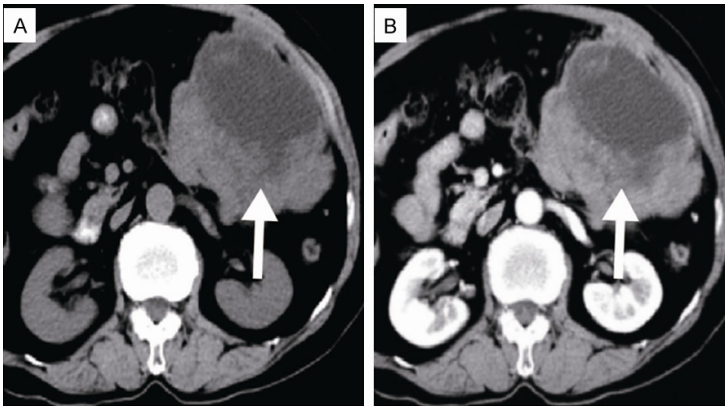


Figure 1. CT findings of pPNETs in soft tissue of the left peritoneal cavity: The tumor showed heterogeneous density and was heterogeneously intense in enhanced scan. A: Plain CT scan; B: Enhanced CT scan.

Hospital from January 2010 to December 2017, with an aim to improve imaging examination of pPNETs and provide experimental evidence for diagnosis and treatment of such patients.

Materials and methods

Study patients

Sixteen patients who had surgically and pathologically confirmed pPNETs and were admitted to The Minhang Branch of Zhongshan Hospital from January 2010 to December 2017 were included in this retrospective study. The patients included 6 males and 10 females, with 9 to 37 years of age (mean, 18.6 ± 2.5 years), and 5 days to 13 months of courses of disease (mean, 6.1 ± 1.4 months). They had the following clinical manifestations: partial pain and pro-

gressive exacerbation (3 cases); perceptible soft tissue masses (4 cases); abdominal pain and distension (2 cases); pelvic pain and lower limb discomfort and numbness (2 cases); fever and cough (1 case); headache, nasal congestion and rhinorrhea or facial numbness (2 cases); neck and shoulder pain, chest and back pain associated with numbness of extremities (2 cases). Among the 16 patients, 8 patients underwent CT plain and enhanced scanning, and 8 MRI plain and enhanced scanning. This study was reviewed and approved by the Medical Ethics Committee of The Minhang Branch of Zhongshan Hospital, and all patients submitted written informed consent.

All patients were followed up by means of telephone calls or outpatient appointments for 2 years. CT and MRI plain and enhanced scans were performed every six month.

Radiological examination

CT examinations were performed on a 64-slice spiral CT scanner (Siemens Somatom Definition AS 128). The parameters were as

follows: 256*256 acquisition matrix, 120 kV voltage, 230 mm*230 mm field of view (FOV), and 5 mm slice thickness and intersection gap. Ultravist (350 mg/ml) was injected with a high-pressure syringe at a dose of 1.5 ml/kg via the antecubital vein at a rate of 2.5 ml/s.

MR examinations were performed on a GE 1.5T signa Excite scanner with images of axial, coronal and Sagittal planes. Conventional MR imaging protocol for lesions included T1-weighted spin-echo imaging (TR/TE, 530/15 ms); T2-weighted fast spin echo imaging (TR/TE, 4800/120 ms). Slice thickness was 4 mm with an intersection gap of 1.5 mm. Gd-DTPA was injected at a dosage of 0.1 mmol in the enhanced MR scan via the anterior elbow vein at a rate of 2.5 ml/s.

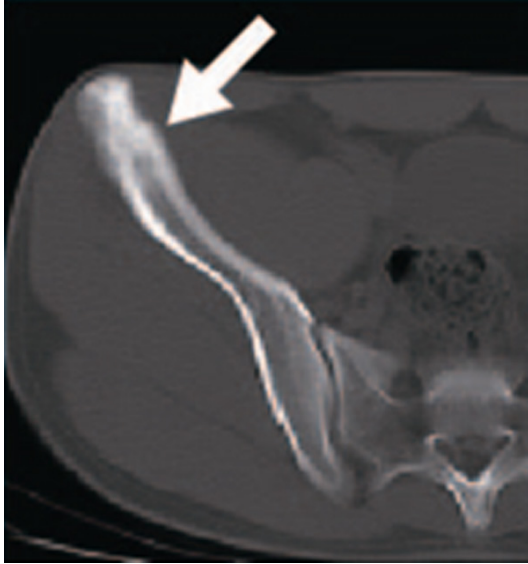


Figure 2. CT findings of pPNETs in bone tissue: osteolytic bone destruction was visible in the right ilium, no periosteal reaction, nor evident surrounding soft tissue masses.

Pathological examination

Samples were surgically removed from all the patients in the study groups, then sampled and prepared into pathological sections. The sections were tested by H&E staining and immunohistochemical staining. Neural markers detected by immunohistochemical staining included CD99, neuron specific enolase (NSE), and S-100 protein. The criteria for diagnosing pPNETs were visible typical undifferentiated small round cells with less cytoplasm, hyperchromatic nuclei, and high ratios of nucleus to cytoplasm, visible nuclear division with or without formation of visible rosettes. Two or more of the mentioned neuronal markers were positively expressed.

Statistical analysis

All the data in this study were analyzed using the SPSS software, version 21.0. Measurement data are described as mean \pm sd, whereas count data was expressed as rates or percentages. $P < 0.05$ was considered significantly different.

Results

Basic characteristics of patients

Of the 16 patients enrolled in this study, the lesions were located in the pelvis in 2 patients,

chest wall in 2 patients, chest cavity in one patient, soft tissue of the lower limbs in 2 patients, spinal canal in 2 patients, paranasal sinuses in 2 patients, abdominal cavity in 2 patients, and osseous tissue in 3 patients. The tumors ranged in volume from $22 \times 15 \times 10 \text{ cm}^3$ to $5 \times 4 \times 3 \text{ cm}^3$, with a mean diameter of $10.4 \times 6.7 \times 5.1 \text{ cm}^3$. One patient was aged younger than 10 years, whereas 9 were 10 to 30 years, 3 were 30 to 50 years, and 3 were older than 50 years. Tumors with well-defined margins were found in 7 patients, and tumors with ill-defined margins in 9 patients. Multiple tumors were observed in 5 patients, and solitary tumor in 11 patients (**Table 1**).

Analysis of CT and MRI features

CT findings of pPNETs in soft tissue showed uneven density with ill-defined margins, necrosis and cystic degeneration, but no calcification. The tumor was significantly heterogeneous in enhanced scan, as shown in **Figure 1**. CT findings of pPNETs in bone tissue presented osteolytic bone destruction with ill-defined margins, no periosteal reaction, with or without surrounding soft-tissue masses (**Figure 2**).

MRI findings of pPNETs in soft tissue showed the lesions were isointense or slightly hypointense to muscle signals on T1WI. On T2WI, the tumor masses revealed heterogeneously hyper-intense or slightly hyper-intense signals. Necrotic or cystic lesions showed changes of longer T1 and long T2 signals. Enhanced scan demonstrated homogeneous or heterogeneous signals, as shown in **Figure 3**. MRI findings of pPNETs in the bone tissue were characterized by disruption of the cortical bone signals in the disrupted regions and changes in the signals in the medullary cavity and surrounding soft tissue. The masses demonstrated slightly hypointense or isointense signals on T1WI, and hyper-intense or slightly hyper-intense signals on T2WI. Enhanced MRI scan demonstrated homogeneous or heterogeneous signals, as seen in **Figure 4**.

Findings of pathological examination

Surgically, the lesions were formed into lobulated or nodular masses of varying sizes, with ill-defined margins with the surrounding tissue and involving the surrounding substantia ossea. Under a light microscope, the tumor cells were small and uniform in size, with less

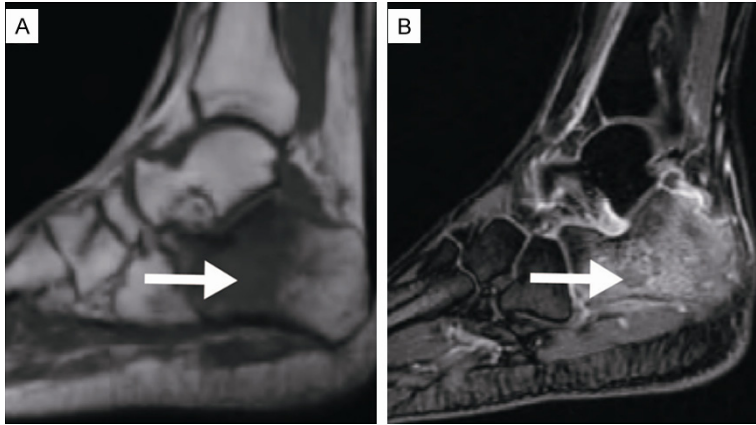


Figure 3. CT findings of pPNETs in soft tissue of left foot: the masses showed ill-defined margins; isointense signals were visible on T1WI and slightly hyper-intense signals on T2WI.

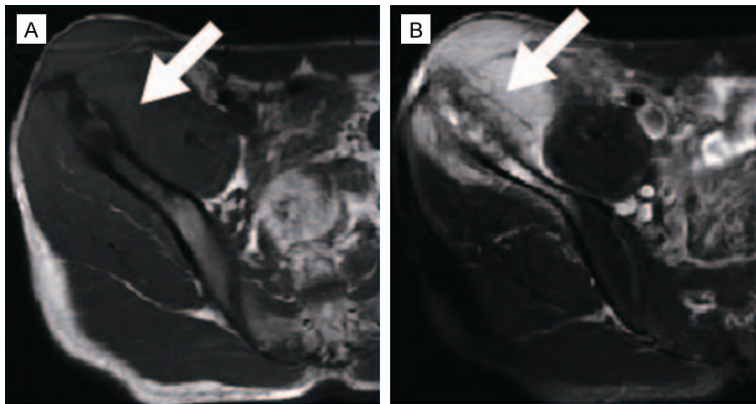


Figure 4. MRI findings of pPNETs in bone tissue: bone destruction was visible in the right ilium, surrounded by evident soft tissue masses; isointense signals were visible on T1WI and slightly hyper-intense signals on T2WI. A: T1WI; B: T2WI.

cytoplasm, common hyperchromatic nuclei and typical Homer-Wright type rosettes (**Figure 5**). Findings of pathological examination of the patient tumors met the criteria for pathological diagnosis of pPNETs.

Recurrence and metastasis analysis

The mean follow-up period was 24.2 ± 2.7 months. After which, 6 patients had recurrent primary lesions, 1 had pulmonary metastasis, 1 had bone metastasis, 1 had intracranial metastasis, and 7 had no recurrence or metastasis after surgery.

Discussion

pPNETs are rare and extremely pernicious malignant tumors [11]. Although they are most

common in children and adolescents, they can also be present in all parts of body of patients at various ages, showing no clinically specific features. Previous studies demonstrate that pPNETs can occur in various organs and the adjacent parts of body, more prevalent in the limbs, chest walls, paravertebral sites [12, 13]. In the present study, clinical data of 16 patients with pPNETs were retrospectively analyzed. The results reveal that the patients ranged in age from 10 to 30 years old (mean, 18.6 ± 2.5 years). The lesions were located in the pelvis (2 cases), chest wall (2 cases), chest cavity (1 case), soft tissue of the lower extremity (2 cases), intraspinal canal (2 cases), paranasal sinuses (2 cases), peritoneal cavity (2 cases), and bone tissue (3 cases). This implied the scattered location and the young age of onset of pPNETs, which is basically consistent with that reported by Kumar et al. [14]. Additionally, the histological features of pPNETs are extraordinarily similar to those of other small round malignant tumors [15, 16]. The 16 cases

of pPNETs enrolled in this study were confirmed by HE staining and neural markers of immunohistochemical staining, which manifested distinct pathological characteristics. Under a light microscope, the cells of pPNETs were small and uniform in size, with less cytoplasm, common karyokinesis, and typical rosettes formation. Immunohistochemical staining confirmed that at least two of the neural markers (including CD99, NSE, Vimentin, S-100, and Syn) were expressed, but malignant schwannomas and neuroblastomas were basically unexpressed, which is consistent with the result of Tan et al. [17].

pPNETs are extremely malignant, invasive, and susceptible to postoperative recurrence and metastasis, with poor prognosis. To improve

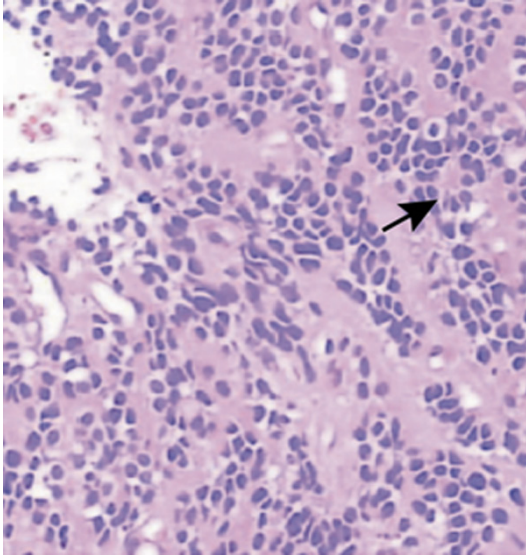


Figure 5. H&E staining of pPNETs (100X). The arrow indicates Homer-Wright type pseudo-rosettes.

radiological diagnosis of pPNETs is clinically significant to guide the treatment of the tumors. However, fewer reports and literature are focused on the CT and MRI features of pPNETs. In the present study, pPNETs of soft tissue presented soft tissue masses of varying degrees, infiltrative proliferation and involving the surrounding tissue. The masses had ill-defined margins and heterogeneous internal density. CT scan showed the masses manifested heterogeneously density, visible cystic degeneration and necrosis. In enhanced scan, the masses showed obvious cystic degeneration and necrosis, and enhanced unevenness. MRI scans revealed iso-intense signals on T1WI, and iso-intense signals on T2WI, and heterogeneously intense signals in enhanced scan. CT findings of pPNETs in bone tissue showed osteolytic bone destruction with ill-defined margins, no periosteal reaction, with or without surrounding soft tissue masses of varying degrees. MRI findings of pPNETs in bone tissue were characterized by discontinuity of the cortical bone signals in the disrupted region and signal changes in the medullary cavity and surrounding soft tissue. The masses presented slightly hypo-intense or isointense signals on T1WI and hyper-intense or slightly hyper-intense signals on T2WI. They were heterogeneously intense in enhanced scan, which is basically consistent with that reported by Duan et al. [18].

pPNETs are mainly treated by surgical resection. A study stated that although postoperative adjuvant radiochemotherapy prolonged the survival time of patients, the rates of local recurrence and metastasis remained high after surgery [19, 20]. In the present study, patients with pPNETs were followed up for 2 years. There were 7 patients without postoperative recurrence or metastasis. Recurrence of primary lesions occurred in 6 patients and tumor metastasis in 3 patients, indicating that the rates of recurrence and metastasis of pPNETs are high.

In conclusion, radiological patterns of pPNETs on CT and MRI scans were specific, but CT and MR examination could display tumor density and signal characteristics, providing reliable evidence for planning of surgical protocols and assessment of therapeutic effects. Nevertheless, there are still some limitations in the present study, such as a small sample size, single center, and unavailability of long-term follow-up results. In the future research, additional multi-center studies with larger sample size and long-term follow-ups are required for further validation.

Disclosure of conflict of interest

None.

Address correspondence to: Hao Wang, Department of Radiology, Minhang Branch, Zhongshan Hospital, Fudan University, No.170, Xinsong Road, Shanghai City 201199, P. R. China. Tel: +86-021-64923400; Fax: +86-021-64923400; E-mail: wang-hao1q2@163.com

References

- [1] Zhang WD and Wu PH. Radiological evaluation of peripheral primitive neuroectodermal tumor arising in abdomen-pelvis region. *Zhonghua Yi Xue Za Zhi* 2008; 88: 3197-3199.
- [2] Yi X, Liu W, Zhang Y, Xiao D, Yin H, Long X, Li L, Zai H, Chen M, Li W and Sun L. Radiological features of primitive neuroectodermal tumors in intra-abdominal and retroperitoneal regions: a series of 18 cases. *PLoS One* 2017; 12: e0173536.
- [3] Dong J, Xing J, Limbu HH, Yue S, Su L, Zhang D and Gao J. CT features and pathological correlation of primitive neuroectodermal tumor of the kidney. *Cell Biochem Biophys* 2015; 73: 59-64.

CT and MRI features of peripheral primitive neuroectodermal tumors

- [4] Li J, Gong P and Guang Z. Three cases of a peripheral primitive neuroectodermal tumor diagnosed using computed tomography or magnetic resonance imaging. *Oncol Lett* 2013; 6: 753-755.
- [5] Ba L, Tan H, Xiao H, Guan Y, Gao J and Gao X. Radiologic and clinicopathologic findings of peripheral primitive neuroectodermal tumors. *Acta Radiol* 2015; 56: 820-828.
- [6] Risi E, Iacovelli R, Altavilla A, Alesini D, Palazzo A, Mosillo C, Trenta P and Cortesi E. Clinical and pathological features of primary neuroectodermal tumor/ewing sarcoma of the kidney. *Urology* 2013; 82: 382-386.
- [7] Jagtap SV, Kale PP, Huddedar A, Hulwan AB and Jagtap SS. Primary primitive neuroectodermal tumor of the kidney. *Indian J Pathol Microbiol* 2018; 61: 252-254.
- [8] Lan B, Wang L, Xu BH and Huang J. The treatment and prognosis of peripheral primitive neuroectodermal tumor. *Zhonghua Zhong Liu Za Zhi* 2017; 39: 850-854.
- [9] Li T, Zhang F, Cao Y, Ning S, Bi Y, Xue W and Ren L. Primary ewing's sarcoma/primitive neuroectodermal tumor of the ileum: case report of a 16-year-old chinese female and literature review. *Diagn Pathol* 2017; 12: 37.
- [10] Tong X, Deng X, Yang T, Yang C, Wu L, Wu J, Yao Y, Fu Z, Wang S and Xu Y. Clinical presentation and long-term outcome of primary spinal peripheral primitive neuroectodermal tumors. *J Neurooncol* 2015; 124: 455-463.
- [11] Kalantari M, Deyhimi P and Kalantari P. Peripheral primitive neuroectodermal tumor (ppnet) of the parotid: report of a rare case. *Arch Iran Med* 2015; 18: 858-860.
- [12] Hou W, Xu L, Zhan H, Wang H, Xu M and Yu Y. Computed tomography and magnetic resonance imaging characteristics of peripheral primitive neuroectodermal tumor: a retrospective analysis of 16 cases. *J Comput Assist Tomogr* 2017; 41: 224-230.
- [13] Qi W, Deng X, Liu T, Hou Y, Yang C, Wu L, Fang J, Tong X, Yang J and Xu Y. Comparison of primary spinal central and peripheral primitive neuroectodermal tumors in clinical and imaging characteristics and long-term outcome. *World Neurosurg* 2016; 88: 359-369.
- [14] Kumar AA and Barodawala S. Peripheral primitive neuroectodermal tumor of cauda equina: a report and review of literature. *Neurol India* 2018; 66: 850-852.
- [15] Singh AK, Srivastava AK, Pal L, Sardhara J, Yadav R, Singh S, Bhaisora KS, Das KK, Mehrotra A, Sahu RN, Jaiswal AK and Behari S. Extraosseous primary intracranial ewing sarcoma/peripheral primitive neuroectodermal tumor: series of seven cases and review of literature. *Asian J Neurosurg* 2018; 13: 288-296.
- [16] Liao YS, Chiang IH and Gao HW. A mesenteric primary peripheral ewing's sarcoma/primitive neuroectodermal tumor with molecular cytogenetic analysis: report of a rare case and review of literature. *Indian J Pathol Microbiol* 2018; 61: 248-251.
- [17] Tan Y, Zhang H, Ma GL, Xiao EH and Wang XC. Peripheral primitive neuroectodermal tumor: dynamic ct, mri and clinicopathological characteristics—analysis of 36 cases and review of the literature. *Oncotarget* 2014; 5: 12968-12977.
- [18] Duan XH, Ban XH, Liu B, Zhong XM, Guo RM, Zhang F, Liang BL and Shen J. Intraspinal primitive neuroectodermal tumor: imaging findings in six cases. *Eur J Radiol* 2011; 80: 426-431.
- [19] Narayanan G, Rajan V and Preethi TR. Primitive neuroectodermal tumors of the kidney. *Proc (Bayl Univ Med Cent)* 2017; 30: 205-208.
- [20] Zhang Y, Cai P, Chen M, Yi X, Li L, Xiao D, Liu W, Li W and Li Y. Imaging findings of adrenal primitive neuroectodermal tumors: a series of seven cases. *Clin Transl Oncol* 2017; 19: 641-649.